NANO LETTERS

xxxx
Vol. 0, No. 0
A−E

Tuning from Thermionic Emission to Ohmic Tunnel Contacts via Doping in Schottky-Barrier Nanotube Transistors

Yung-Fu Chen and Michael S. Fuhrer*

Department of Physics and Center for Superconductivity Research, University of Maryland, College Park, Maryland 20742-4111

Received June 15, 2006; Revised Manuscript Received July 17, 2006

ABSTRACT

Electrical power >1 mW is dissipated in semiconducting single-walled carbon nanotube devices in a vacuum. After high-power treatment, devices exhibit lower on currents and intrinsic, ambipolar behavior with near-ideal thermionic emission from Schottky barriers of height one-half the band gap. Upon exposure to air, devices recover p-type behavior, with positive threshold and ohmic contacts. The air-exposed state cannot be explained by a change in contact work function but instead is due to doping of the nanotube.

Semiconducting single-walled carbon nanotubes (s-SWNTs) have advantageous materials properties for field-effect transistor (FET) applications: intrinsic nanoscale dimensions (i.e., "ultrathin body"),[1] high mobility,[2] and high carrier velocity.[3] As-fabricated s-SWNTs in an FET geometry (SWNT-FETs) are typically found to be p-type, and doping, either from the electrodes[4] or chemical species[5] such as adsorbed oxygen,[6] was originally assumed to be the cause. Later the group of Avouris et al. posited that p- vs n-type behavior was determined entirely by the SWNT/electrode interface[7,8] and explicitly rejected doping. Avouris et al. modeled the (short-channel) s-SWNT-FET as a ballistic Schottky barrier FET (SB-SWNT-FET), in which the conductance is modulated by the gate field through narrowing of the SBs through which electrons tunnel.[7] SB-SWNT-FETs thus display unusual vertical scaling,[9] large subthreshold swings,[2,8] and ambipolar behavior.[3,10,11] Even though they rely on tunneling, high on currents may be realized in SB-SWNT-FETs with thin gate dielectrics, due to the nanoscale diameter of s-SWNTs and their small effective mass. More recently negative SB height "ohmic" contacts to nanotubes have been established through the use of other metals (e.g., Pd)[12] and provide another route to high on currents and additionally provide near-ideal subthreshold swings.

In this Letter, we show that doping provides a third route to obtain high on currents in a SWNT-FET. Modest doping of the SWNT narrows the SBs and provides a high-conductance tunnel contact from electrode to SWNT. This tunnel contact is "ohmic": in the on state its conductance does not depend strongly on temperature or gate or drain voltages,[13] though in the off state it provides poor subthreshold swings.[1]

High electrical bias (up to ±50 V) is applied to chemical vapor deposition (CVD) grown s-SWNT devices in a vacuum, causing electrical heating due to high power dissipation (>1 mW) in the devices. After heating, the s-SWNTs are intrinsic, ambipolar, and show significantly lower on currents. The conductance is thermally activated, with an activation energy approximately half the band gap, consistent with SB-SWNT-FET behavior in a thick dielectric device with midgap alignment of the metal Fermi level. Upon exposure to air, the s-SWNTs recover high on current, positive threshold, and p-type behavior. However, air-exposed devices retain large subthreshold swings, and the n-type conduction is comparable to the heat-treated devices in a vacuum. We conclude that our SWNT-FETs in ambient are p-doped SB-SWNT-FETs and exhibit high on currents due to thinning of the SB by doping of the SWNT.

SWNTs were grown using a CVD process, and device fabrication is the same as that described in our previous publication.[3] The measured nanotube diameters d range from 1.6 to 4.2 nm, with most around 2 nm. Metal contacts were formed by thermally evaporating 1.2 nm Cr and 100 nm Au. Devices were annealed at 400 °C under Ar and H_2 flow for 3 min. The nanotube length between the contacts L ranges from one to tens of micrometers, larger than dielectric thickness t (500 nm SiO_2) and contact thickness. Electrical measurements were performed by grounding the source electrode ($V_s = 0$) and applying V_d to the drain, and V_g to the gate, while measuring the drain current I_d in a ^{4}He cryostat or in ambient environment.

Figure 1 shows V_d up to ±50 V applied to a s-SWNT (d = 2.2 nm and $L = 9$ μm) device at $V_g = 0$. The device

* Corresponding author. Tel: (301) 405-6143. Fax: (301) 314-9465. E-mail: mfuhrer@physics.umd.edu. Web: http://www.physics.umd.edu/condmat/mfuhrer/.

10.1021/nl061379b CCC: $33.50
Published on Web 07/27/2006

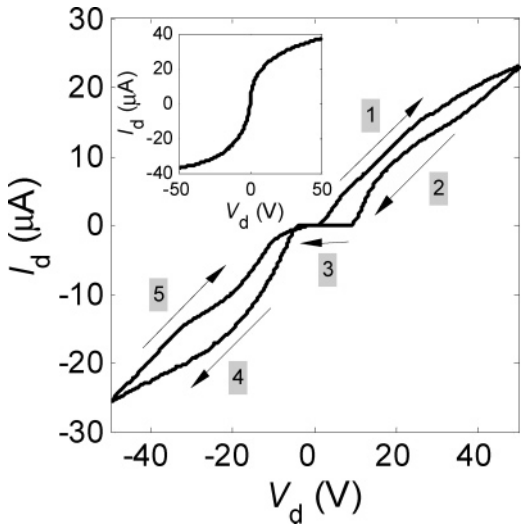

Figure 1. Drain current I_d vs drain voltage V_d for SWNT devices. Main panel shows I_d vs V_d for a semiconducting SWNT with V_d up to ±50 V at $V_g = 0$ and $T = 1.4$ K. The arrows and numbers indicate sweep directions and sequence of sweeps of V_d. Inset is I_d vs V_d for the same V_d range for a m-SWNT device ($d = 2.0$ nm and $L = 9$ μm) at $T = 5$ K. (In this case a gate voltage $V_g = V_d/2$ was applied during the sweep of V_d.)

conducts well originally at low bias (sweep 1). After large V_d (sweep 1) is applied, the conductivity is lower when V_d is ramped down (sweep 2) compared with sweep 1. A low-conductance gap of width ~10 V is seen in the low-bias region when V_d returns to small values (sweep 3). This gap at low bias due to the application of high V_d is irreversible while the device remains in a vacuum; the original conductance at zero gate voltage cannot be recovered by application of V_g or V_d; it is different from the previously observed hysteresis[14] in SWNT-FETs due to charge trapping in the gate dielectric. The original conductance at zero gate voltage is completely recovered when the device is exposed to atmospheric gas (not shown). The device can be cycled between these two states (which we will refer to as "high-conductance state" and "low-conductance state") repeatedly by applying high V_d or exposing it to air. Applying large V_d to metallic SWNT (m-SWNT) devices does not change the I_d-V_d characteristic (see inset, Figure 1).

Figure 2 depicts transfer curves of the same s-SWNT device at different temperatures T in the high-conductance state (Figure 2A) and in the low-conductance state (Figure 2B). The device shows ambipolar behavior in both states (see inset, Figure 2A)[3,11] but in the low-conductance state the ambipolar behavior is very symmetric; at all temperatures the hole and electron on currents are the same order of magnitude, and the subthreshold swings, S, are similar. Around $V_g = 0$ (-3 V $< V_g <$ 3 V), S values for holes and electrons are very large (on order 10 V/decade), and the current decreases very quickly with temperature.

We first examine the temperature dependence of the conductance in the low-conductance state in the region near $V_g = 0$. Figure 3 shows the data from Figure 2B at several V_g values on an Arrhenius plot. An effective activation energy E_a can then be extracted. Figure 4 shows E_a as a function of V_g; over a large range (-3 V $< V_g <$ 3 V) E_a has a fairly

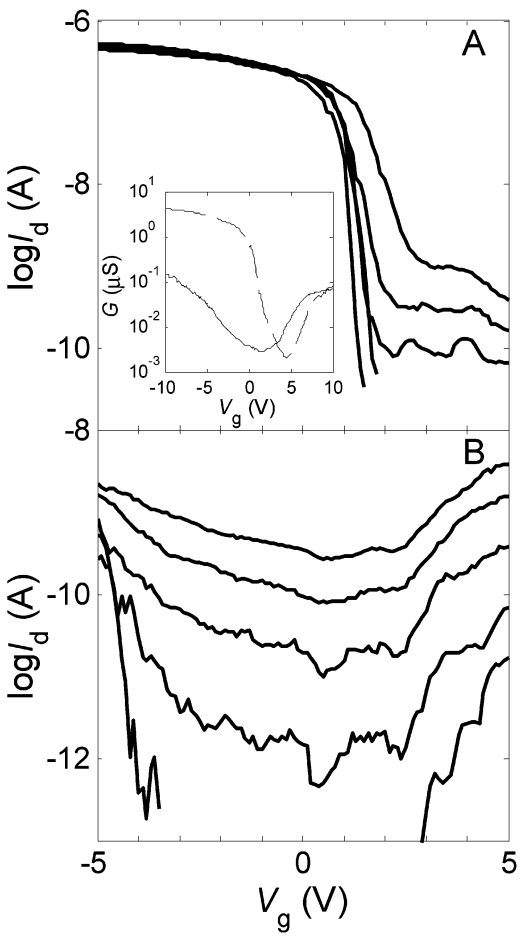

Figure 2. Transfer characteristics of a s-SWNT device. Main panels: (A) high-conductance state; (B) low-conductance state. The five curves in both main panels are at $T = 300$, 250, 200, 150, and 100 K from top to bottom, respectively, and $V_d = 0.1$ V. Inset of (A): Conductance vs V_g at $T = 300$ K (the dashed and solid lines are taken in the high-conductance state and the low-conductance state, respectively).

constant value of ~150 meV, with a maximum ~170 meV, and is similar for electrons ($V_g > 0$) and holes ($V_g < 0$). The estimated energy gap for this nanotube of diameter $d =$ 2.2 nm is $E_g = 380$ meV.[15,16] (The band gap is calculated assuming a tight-binding nearest-neighbor overlap integral of 2.89 eV obtained from Raman spectroscopy.[15,16]) We interpret E_a as the SB height,[17] which is similar for electrons and holes, indicating midgap alignment of the metal Fermi level. Such a midgap alignment is consistent with the fact that the work function of chromium (4.5−4.7 eV[18−20]) is very similar to that of theoretical estimates[21] and experimental measurements[22] for large-diameter isolated SWNTs (~4.7 eV). The SB height should therefore be $E_g/2$. E_a indeed approaches the expected value $E_g/2 = 190$ meV, as expected in the limit of an intrinsic SWNT on thick dielectric.[17] We conclude that the low-conductance state corresponds to an intrinsic s-SWNT with symmetric SBs for electrons and holes.

It is worth discussing here why we can successfully measure the SB height using the thermionic emission model. Due to the competition between tunneling and thermionic emission, the measured activation energy should be less than

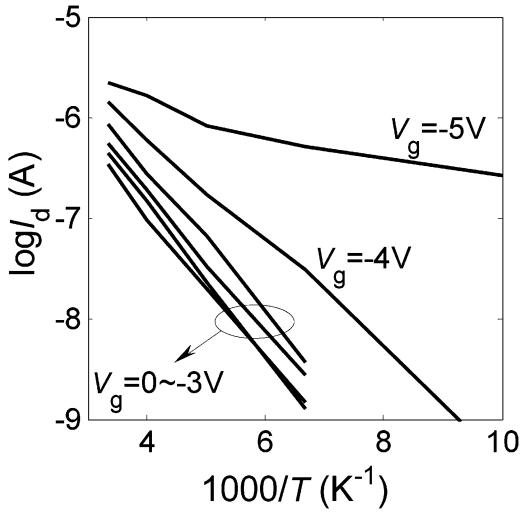

Figure 3. Arrhenius plot of the current at various gate voltages from data of Figure 2B. The six curves represent V_g values ranging from −5 to 0 V, in steps of 1 V.

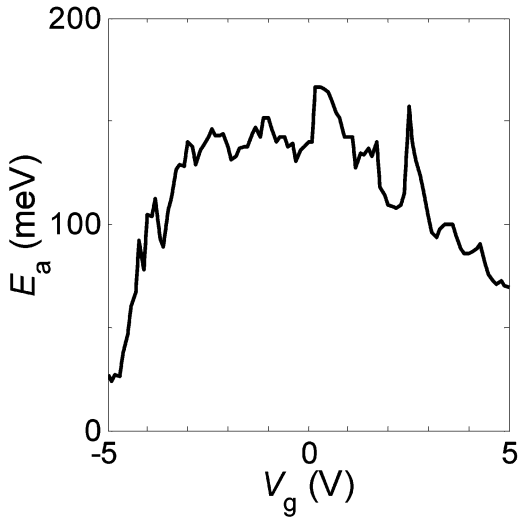

Figure 4. Activation energy E_a vs gate voltage V_g derived from data of Figure 3.

the true SB height. However, as pointed out in ref 17, thermionic emission dominates in the limit of an intrinsic SWNT at low V_g on a thick gate dielectric, which are constraints well-satisfied in our devices, and thus the activation energy should approximate the true SB height here. As will be shown below, the thermionic-emission limit could not be previously observed in SB-SWNT-FETs on thick dielectric due to doping of the SWNT leading to increased tunneling through the SBs.

We now turn to the high-conductance state produced by exposure to air. As seen in the inset of Figure 2A, the device has higher on current in the p-type region compared to the low-conductance state, while on current in the n-type region is nearly unchanged. The subthreshold swing in the p-type region is smaller than that in the low-conductance state but still much larger than the k_BT ln10/$e \approx 60$ mV/decade (k_B is Boltzmann's constant and e is the electronic charge) expected for an ideal MOSFET at room temperature.[23] The off current is nearly identical to that in the low-conductance state. We

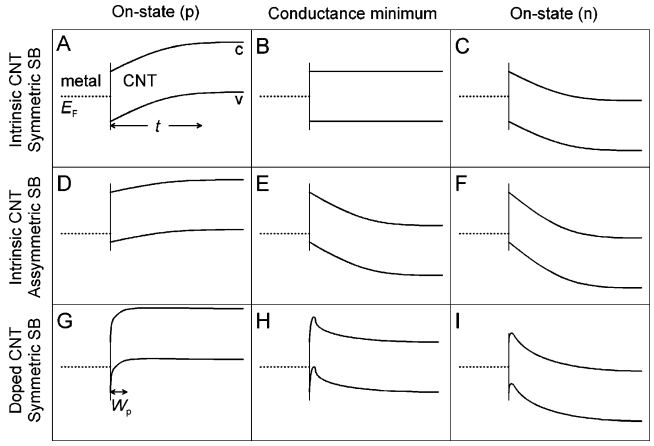

Figure 5. Band diagrams for a SB-SWNT-FET. (A−C) Band diagrams for an intrinsic (undoped) SB-SWNT-FET with equal height SBs at negative gate voltage (A), near zero gate voltage (B), and positive gate voltage (C). The width of the SB is roughly the gate oxide thickness t. The conductance minimum (B) occurs at the flat band condition, when barriers for electrons and holes are equal. (D−F) Band diagrams for an intrinsic SB-SWNT-FET with unequal height SBs. The width of the SB is again roughly the gate oxide thickness t. The on state for p-type conduction (D) has a smaller SB height for holes than that in (A), resulting in higher current. The conductance minimum (E) occurs at more positive V_g than the flat band condition, when barriers for electrons and holes are roughly equal in height, and larger than those in (B), resulting in a lower minimum current. The on state for n-type conduction (F) has a larger SB height for electrons than that in (C), resulting in lower current. (G−I) Band diagrams for a hole-doped SB-SWNT-FET with equal height SBs. The width of the SB for negative gate voltage (G) is determined by W_p, the doping depletion length, resulting in higher current than that in (A). At the conductance minimum (H) the barriers for electrons and holes are similar in height to those in (B), except within a short distance W_p of the interface where the additional barrier for electrons is largely transparent to tunneling, resulting in a similar minimum current. In the on state for n-type conduction (I), the electron density is similar to (C), and thus the barrier for electrons is similar in shape, except within a short distance W_p of the interface, resulting in a similar n-type current. Note that (H) and (I) occur at more positive V_g than (B) and (C), respectively, due to the doping of the SWNT.

explore two possible explanations for the hole conduction enhancement observed upon air exposure: the metal electrode work function is increased, or the nanotube is doped.

Increase in metal work function should result in the following effects. First, n-type conduction should be suppressed because of increasing SB height for electrons (see Figure 5F).[7] In contrast, Figure 2A (inset) shows that n-type conductance is nearly identical in the high- and low-conductance states. Second, the off current (minimum current) should decrease exponentially as the barrier for electrons increases (see Figure 5E), which is also not seen. Therefore, we rule out metal contact work function change as the explanation for the high-conductance state.

In contrast, p-type chemical doping of s-SWNTs upon air exposure can explain our experimental results. Chemical doping not only increases free carriers in nanotubes but also changes the SB thickness by varying the depletion width W_p.[24] The depletion width for nanotubes varies exponentially with inverse doping density D_p; $W_p \approx d/2 \exp(2\epsilon\epsilon_0 E_g/e^2 d N D_p)$,[24] where ϵ_0 is the electric constant, $\epsilon \approx 2.45$ the

average dielectric constant of the oxide and vacuum, and $N \approx 38\ nm^{-2}$ is carbon atoms per unit surface area. In Figure 2A, the gate voltage needed to remove all the carriers is ~1.6 V. Assuming a gate capacitance per length $c_g \approx 0.20$ pF/cm in our device geometry,[2,3] we estimate the doping level D_p is about $2.0 \times 10^6\ cm^{-1} \approx 7.6 \times 10^{-4}$ holes/carbon. Then $W_p \approx 5.5$ nm, which is at least 1 order of magnitude smaller than the SB thickness controlled by electrostatic gating in our device geometry.[7,25] The thin SB due to a thin depletion width and the unchanged SB heights for both valence and conduction bands easily explains why the on current is enhanced in p-type conduction (see Figure 5G), while the off current is not changed in the high-conductance state compared with the low-conductance state (see Figure 5H). Because of the unchanged SB heights for both valence and conduction bands in the high-conductance state, the ambipolar characteristics are preserved (see Figure 5I). Note that in the high-conductance state, the temperature dependence of the conductance at negative V_g is small or negligible, and the measured activation energy is much smaller than that in the low-conductance state. This arises not because of a reduction in SB height for holes (which would necessitate an increase in SB height for electrons) but rather due to tunneling dominating thermionic emission as the SB is thinned by hole-doping; doping enhances the tunneling contribution, lowering the measured activation energy compared to the true SB height.[17] This explains the failure of previous experiments to observe the expected thermionic emission and measure the correct SB height in SB-SWNT-FETs on thick dielectric.[10] Also, the off current in the high-conductance state occurs at more positive V_g compared with the low-conductance state (see inset of Figure 2A), which is another verification that the device is hole-doped in the high-conductance state.

The exact nature of the chemical doping remains unclear. The obvious possibility is that oxygen adsorbs on the s-SWNTs, accepting electrons. Oxygen is known to affect the thermopower and resistivity of bulk SWNT samples.[6] Jhi et al.[26] predicted that adsorbed O_2 donated 0.1 hole per adsorbed molecule to the SWNT. However, a recent paper[27] exploring s-SWNTs with one section suspended across a trench found that the s-SWNT section bound on the SiO_2 substrate is p-type doped (with a similar doping magnitude observed here), and the suspended s-SWNT is undoped; this raises the possibility that SWNT doping arises from an interaction with the SiO_2 substrate. For solution-processed SWNTs on Au electrodes, annealing produced n-type FETs, and exposure to O_2 restored p-type operation, interpreted there as due to changes in metal work function.[28] However, the origin of n-type behavior in the annealed FETs remains unclear, so a complete picture is lacking.

We have made a preliminary investigation of the effect of various gases on the device when in the low conductance state. Exposure of the device to dry N_2, O_2, or He did not alter the low conductance state, while exposure to humid air immediately caused a change to the high conductance state, suggesting that water is necessary for doping. While it is possible that doping may arise via direct interaction between water and the SWNT, we consider it more likely that the surface charge of the SiO_2 in the presence of pure water[29] dopes the SWNT or water is necessary for O_2 doping. The latter is consistent with the observation that water is necessary to observe doping of SWNTs by ammonia,[30] so it is possible that O_2 doping only occurs in the presence of an adsorbed water layer. Carefully controlled experiments in ultrahigh vacuum to separate the effect of water exposure from O_2 exposure are underway.

In conclusion, we have shown that dissipating high power in a SWNT-FET can reveal its intrinsic undoped behavior. In ambient environment, s-SWNTs on SiO_2 substrates are doped, and such chemical doping allows ohmic contacts and high on currents in SB-SWNT-FETs. It is notable that the effects demonstrated here also form the basis of an electronically programmable FET: application of a high electrical current is sufficient to reduce the on current by 2 orders of magnitude and effectively remove a particular FET from a circuit.

Acknowledgment. This material is based upon work supported by the National Science Foundation under Grant No. 0102950, and the UMD-MRSEC shared equipment facilities were used in this work. The authors are thankful for useful discussions with David Tobias and Masa Ishigami.

References

(1) Rahman, A.; Guo, J.; Datta, S.; Lundstrom, M. S. *IEEE Trans. Electron Devices* **2003**, *50* (9), 1853−1864.
(2) Durkop, T.; Getty, S. A.; Cobas, E.; Fuhrer, M. S. *Nano Lett.* **2004**, *4* (1), 35−39.
(3) Chen, Y. F.; Fuhrer, M. S. *Phys. Rev. Lett.* **2005**, *95* (23), 236803.
(4) Tans, S. J.; Verschueren, A. R. M.; Dekker, C. *Nature* **1998**, 393 (6680), 49−52.
(5) Martel, R.; Schmidt, T.; Shea, H. R.; Hertel, T.; Avouris, P. *Appl. Phys. Lett.* **1998**, *73* (17), 2447−2449.
(6) Collins, P. G.; Bradley, K.; Ishigami, M.; Zettl, A. *Science* **2000**, *287* (5459), 1801−1804.
(7) Heinze, S.; Tersoff, J.; Martel, R.; Derycke, V.; Appenzeller, J.; Avouris, P. *Phys. Rev. Lett.* **2002**, *89* (10), 106801.
(8) Appenzeller, J.; Knoch, J.; Derycke, V.; Martel, R.; Wind, S.; Avouris, P. *Phys. Rev. Lett.* **2002**, *89* (12), 126801.
(9) Wind, S. J.; Appenzeller, J.; Martel, R.; Derycke, V.; Avouris, P. *Appl. Phys. Lett.* **2002**, *80* (20), 3817−3819.
(10) Martel, R.; Derycke, V.; Lavoie, C.; Appenzeller, J.; Chan, K. K.; Tersoff, J.; Avouris, P. *Phys. Rev. Lett*. **2001**, *87* (25), 256805.
(11) Radosavljevic, M.; Heinze, S.; Tersoff, J.; Avouris, P. *Appl. Phys. Lett.* **2003**, *83* (12), 2435−2437.
(12) Javey, A.; Guo, J.; Wang, Q.; Lundstrom, M.; Dai, H. *Nature* **2003**, *424*, 654−657.
(13) Yaish, Y.; Park, J. Y.; Rosenblatt, S.; Sazonova, V.; Brink, M.; McEuen, P. L. *Phys. Rev. Lett.* **2004**, *92* (4), 046401.
(14) Fuhrer, M. S.; Kim, B. M.; Durkop, T.; Brintlinger, T. *Nano Lett.* **2002**, *2* (7), 755−759.
(15) Dresselhaus, M. S.; Dresselhaus, G.; Eklund, P. C., *Science of fullerenes and carbon nanotubes*; Academic Press: San Diego, CA, 1996.
(16) Souza-Filho, A. G.; Jorio, A.; Hafner, J. H.; Lieber, C. M.; Saito, R.; Pimenta, M. A.; Dresselhaus, G.; Dresselhaus, M. S. *Phys. Rev. B* **2001**, *63* (24), 241404-4.
(17) Appenzeller, J.; Radosavljevic, M.; Knoch, J.; Avouris, P. *Phys. Rev. Lett.* **2004**, *92* (4), 048301.
(18) Wahlin, H. B. *Phys. Rev.* **1948**, *73* (12), 1458.
(19) Lapeyre, G. J.; Kress, K. A. *Phys. Rev.* **1968**, *166* (2), 589.

(20) Eastman, D. E. *Physi. Rev. B* **1970**, *2* (1), 1.
(21) Zhao, J. J.; Han, J.; Lu, J. P. *Phys. Rev. B* **2002**, *65* (19), 193401.
(22) Cui, X. D.; Freitag, M.; Martel, R.; Brus, L.; Avouris, P. *Nano Lett.* **2003**, *3* (6), 783−787.
(23) Sze, S. M. *Physics of semiconductor devices*, 2nd ed.; New York, 1981.
(24) Leonard, F.; Tersoff, J. *Phys. Rev. Lett.* **1999**, *83* (24), 5174−5177.
(25) Odintsov, A. A. *Phys. Rev. Lett.* **2000**, *85* (1), 150−153.
(26) Jhi, S. H.; Louie, S. G.; Cohen, M. L. *Phys. Rev. Lett.* **2000**, *85* (8), 1710−1713.
(27) Minot, E. D.; Yaish, Y.; Sazonova, V.; McEuen, P. L. *Nature* **2004**, *428*(6982), 536−539.
(28) Derycke, V.; Martel, R.; Appenzeller, J.; Avouris, P. *Nano Lett.* **2001**, *1*(9), 453−456.
(29) Behrens, S. H.; Grier, D. G. *J. Chem. Phys.* **2001**, *115* (14), 6716−6721.
(30) Bradley, K.; Gabriel, J. C. P.; Briman, M.; Star, A.; Gruner, G. *Phys. Rev. Lett.* **2003**, *91* (21), 218301.

NL061379B